

See discussions, stats, and author profiles for this publication at: <https://www.researchgate.net/publication/280022402>

# Zeolite-like sorption of volatile organics in $\beta$ -[CuL<sub>2</sub>] (L = {CF<sub>3</sub>COCHCOC(CH<sub>3</sub>)<sub>2</sub>OCH<sub>3</sub>}-)

ARTICLE · DECEMBER 2000

CITATIONS

20

READS

12

## 4 AUTHORS:



[Andrey Yu Manakov](#)

Russian Academy of Sciences

**116** PUBLICATIONS **1,055** CITATIONS

[SEE PROFILE](#)



[Dmitriy Soldatov](#)

University of Guelph

**103** PUBLICATIONS **1,832** CITATIONS

[SEE PROFILE](#)



[John A. Ripmeester](#)

National Research Council Canada

**713** PUBLICATIONS **15,592** CITATIONS

[SEE PROFILE](#)



[Janusz Stanisław Lipkowski](#)

Cardinal Stefan Wyszyński University in Wars...

**338** PUBLICATIONS **3,110** CITATIONS

[SEE PROFILE](#)

# Zeolite-Like Sorption of Volatile Organics in $\beta$ -[CuL<sub>2</sub>] (L = {CF<sub>3</sub>COCHCOC(CH<sub>3</sub>)<sub>2</sub>OCH<sub>3</sub>}<sup>−</sup>)<sup>†</sup>

A. Yu. Manakov,<sup>‡</sup> D. V. Soldatov,<sup>‡,§</sup> J. A. Ripmeester,<sup>\*,§</sup> and J. Lipkowski<sup>#</sup>

*Institute of Inorganic Chemistry, Siberian Branch of the Russian Academy of Sciences, Novosibirsk 630090, Russia, Steacie Institute for Molecular Sciences, National Research Council of Canada, Ottawa K1A 0R6, Canada, and Institute of Physical Chemistry, Polish Academy of Sciences, Warszawa 01 224, Poland*

Received: April 13, 2000; In Final Form: September 20, 2000

The  $\beta$ -form of the title copper(II) acetylacetonate derivative shows zeolite-like behavior, as exemplified by its ability to absorb volatile guests instantly and reversibly over a wide range of guest pressures. Sorption isotherms with methylene chloride, chloroform, carbon tetrachloride, *n*-pentane, acetone, tetrahydrofuran, and diethyl ether were determined at 30 °C or over a range of temperatures. For all guests tested, sorption occurred even at minimal guest pressure, indicating the presence of porosity of the host sorbent even without included species present. The nature of the isotherms as well as other characteristics suggests a physical mode of sorption on the inner hydrophobic surface of the host pores. With increasing pressure, the isotherms quickly reached plateau values corresponding to a guest/host ratio of 2/3 for compact molecules and to a lower value for *n*-pentane and diethyl ether. At elevated temperatures and low guest pressure, the porous  $\beta$ -form collapses to the dense,  $\alpha$ -form of the complex, as does the guest-free  $\beta$ -form. At 70 °C, the enthalpy of the  $\alpha$ -to- $\beta$  transformation equals 1.31(5) kJ/mol as determined from DSC experiments. In the  $\beta$ -[CuL<sub>2</sub>]-\*2/3(chloroform) compound studied by X-ray diffraction, 1D channel segments of both larger and smaller widths are filled stoichiometrically with guest species, thus explaining the limiting guest–host ratio observed.

## Introduction

Since sorbents that mimic zeolites were first reported,<sup>1</sup> such “organic zeolite analogs” have evoked an ever-increasing interest.<sup>2,3</sup> “Zeolite-like” behavior implies the permanent porosity of a sorbent as shown by its ability to absorb, instantly and reversibly, large amounts of appropriate guest material even at a minimal guest pressure. Originally, the “organic” label was used to stress the hydrophobic nature of the interior pore surface rather than the organic nature of the host. Thus, although the first representatives of “organic zeolite analogs” were built up from metal complexes, the “organic nature” of the micropores revealed itself clearly by the inability to absorb water and by the special shape of the adsorption isotherm for highly polar guests.<sup>1</sup>

Recently,<sup>4,5</sup> we reported on a new metal complex with a permanent pore structure,  $\beta$ -[CuL<sub>2</sub>] (L = {CF<sub>3</sub>COCHCOC(OMe)Me<sub>2</sub>}<sup>−</sup>). The molecule of this modified copper(II) acetylacetonate has two peripheral methoxy-oxygen donors that coordinate to copper atoms of neighboring molecules, thus building up a 3D polymer with isolated straight channels of ca. 6 Å in diameter (Figure 1). Although the microporous  $\beta$ -form is metastable with respect to the dense,  $\alpha$ -polymorph of the complex, it remains intact even after complete removal of the guest component (as unequivocally proved by powder X-ray diffraction and helium pycnometry<sup>4</sup>). Such a remarkable robust-

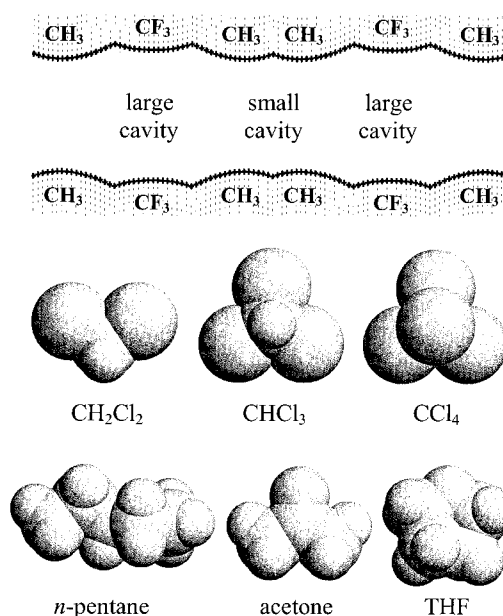


**Figure 1.** Profile of the 1D channel in  $\beta$ -[CuL<sub>2</sub>]\*2/3(benzene)<sup>4</sup> with the designated location of large and small cavities and van der Waals dimensions of the guests studied given on the same scale for comparison. A channel segment of two periods is shown.

ness was attributed to the fact that phase interconversion requires trans-cis isomerization of a number of the Cu chelate building blocks.<sup>4</sup>

This paper elucidates further the zeolite-like mode of inclusion into the  $\beta$ -form. Sorption isotherms were determined and compared for seven guests differing in size, shape, and polarity.

<sup>†</sup> Issued as NRCC No. 43849.

<sup>\*</sup> To whom correspondence should be addressed. Fax: (613) 998-7833. E-mail: jar@ned1.sims.nrc.ca.

<sup>‡</sup> Institute of Inorganic Chemistry.

<sup>§</sup> Steacie Institute for Molecular Sciences.

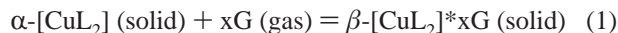
<sup>#</sup> Institute of Physical Chemistry.

Figure 1 shows the channel profile (as found in the benzene inclusion<sup>4</sup>) with the hydrophobic inner surface formed by methyl and trifluoromethyl groups. There are segments of different widths referred to as large and small cavities, respectively. The ideal guest–host stoichiometry is 2/3 provided each cavity, both large and small, is filled with one guest molecule (another option is a 1/3 stoichiometry arising from a filling of only large cavities<sup>6</sup>). Van der Waals dimensions of the guests studied are given in the same figure for comparison (diethyl ether is not shown as it is very near to *n*-pentane in size). Other work reported here includes the relative stability of the dense  $\alpha$ - and porous  $\beta$ -polymorphs and the crystal structure of the inclusion with chloroform with an ideal stoichiometry of 2/3.

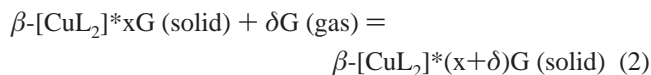
## Experimental Section

**Isotherms.** The isotherms were determined with a Mettler AE100 balance and an external reservoir of guest vapor, as described in ref 7. The temperature in the apparatus was maintained with an accuracy of 0.5 °C, and the pressure was measured with a mercury manometer with an accuracy of  $\pm 0.5$  mmHg. The original samples consisted of 200 mg of pure  $\alpha$ -form sifted through a 0.05-mm sieve. The weight increase varied from 12 mg for *n*-pentane and diethyl ether to 37 mg for carbon tetrachloride. The experimental error in the mass changes was 0.5 mg from where the error for maximum guest–host ratios  $x$  is from 1–4%.

The first point in each experiment was obtained at the maximum guest vapor pressure to transform the entire sample to the  $\beta$ -form:



After the sample weight stabilized, the guest pressure was decreased stepwise by pumping to obtain the entire isotherm under desorptive conditions (reverse of reaction 2). After that, the pressure was increased again to obtain one or more points for the “forward” reaction:



Although the “forward” reaction was an order of magnitude slower, lasting an hour or more, the results corresponded within experimental error to those of the “reverse” process. Reversibility is demonstrated for all isotherms (Figures 2–7) using points with bars below or above, indicating the approach to equilibrium by guest pressure increase or decrease, respectively. Some “understated”  $x$ -values for the forward process may be explained by the achievement of a “pseudo-equilibrium” state, as also observed for a Werner complex zeolite analogue.<sup>8</sup> The most serious problems were noted for the carbon tetrachloride isotherms which were compiled essentially from the “reverse” points.

Two or more independent runs were performed to determine each isotherm. No significant changes among parallel runs were observed. The reproducibility is illustrated in Figures 2 and 3, showing data of four experimental series. At the same time, we do not exclude systematic errors due to adsorption on developed surfaces of the host material or in mesopores. This contribution could be of the order of a percent.

**Preparations, Phase Control and DSC-Measurements.** A full description of the synthesis of the title complex was given in our previous work.<sup>4</sup> The sublimed  $\alpha$ -form (dense polymorph) was used as starting material for isotherm determinations. Phase

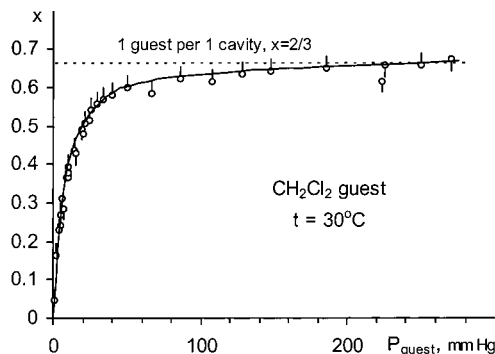


**Figure 2.** The sorption isotherm (30 °C) of methylene chloride in  $\beta$ -[CuL<sub>2</sub>] (four experimental series). Low bars indicate points approaching equilibrium from low guest pressures, whereas the high bars indicate points obtained in the reverse direction.

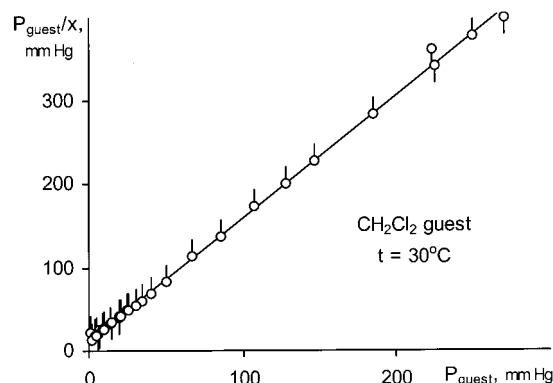


**Figure 3.** The methylene chloride isotherm (see Figure 2) given in Langmuir coordinates. The equation for the least-squares minimized line is  $P_{\text{guest}}/x = 1.48(1) P_{\text{guest}} + 12(1)$ .

checks of samples were made with a Rigaku Geigerflex diffractometer (Co  $K\alpha$ -radiation,  $\lambda = 1.7902$  Å). Powder patterns were recorded in the 5–15° 2 $\theta$ -range where the  $\alpha$ -form has strong reflections at 11.0° (002 + 111) and 14.1° (021 + 200), whereas the  $\beta$ -form has strong reflections at 8.4° (–120), 13.8° (021), and 14.6° (030) (reference diffractograms are shown in Figure 8; for full diffractograms see ref 4).

The empty  $\beta$ -form used in DSC measurements was prepared as described before<sup>4</sup> but using methylene chloride as the transforming agent. Samples of  $\alpha$ -[CuL<sub>2</sub>] (0.5 g) were exposed to methylene chloride vapor (300 mmHg) for 5 h at room temperature, and, after that, the reaction vessel was pumped out down to  $10^{-5}$  mmHg for 12 h. Recovered samples showed pure  $\beta$ -structure with a guest residue of less than 0.1 mass %. DSC-measurements were performed using 2920 Modulated Differential Scanning calorimeter (TA Instruments). Samples of 5–10 mg were pressed inside aluminum pans and the DSC curves were recorded at a 5°/min heating rate. To reduce systematic errors, samples of each polymorph were used from three independent syntheses, and the calorimeter was calibrated before each run.

**Crystallography.** Of all compounds studied, only that with chloroform was studied crystallographically. Crystals included with methylene chloride instantly lost a large portion of guest when taken out from under the mother liquor. Crystals included with carbon tetrachloride become unsuitable for single-crystal X-ray measurements because of spontaneous cracking in air. Inclusions with light guests were undesirable because of problems locating guest molecules that are disordered over six symmetrically equivalent sites arising from the  $R\bar{3}$  axis in the channel.

**TABLE 1: Details of the Structural Determination and the Main Parameters for the Structure**

formula	$\beta$ -[CuL <sub>2</sub> ]*2/3(chloroform)
gross formula	C <sub>16</sub> H <sub>20</sub> CuF <sub>6</sub> O <sub>6</sub> *(CHCl <sub>3</sub> ) <sub>0.67</sub>
formula weight	565.4
temperature, °C	−100
crystal system	trigonal
space group	<i>R</i> 3̄ (no 148)
unit cell parameters:	
<i>a</i> , Å	24.111(4)
<i>c</i> , Å	10.491(2)
<i>V</i> , Å <sup>3</sup>	5282(2)
<i>Z</i>	9
calculated density, g cm <sup>−3</sup>	1.600
absorption coefficient (Mo <i>K</i> α), cm <sup>−1</sup>	12.34
no. of unique reflections:	
used ( <i>I</i> > 0)	3045
intense ( <i>I</i> > 2σ( <i>I</i> ))	2674
no. of refined parameters	263
<i>R</i> -values:	
<i>R</i> <sub>int</sub> (all data)	0.032
<i>R</i> 1 = Σ    <i>F</i> <sub>o</sub>   −   <i>F</i> <sub>c</sub>   /Σ   <i>F</i> <sub>o</sub>   (intense data)	0.034
<i>wR</i> 2 (intense data)	0.098
goodness-of-fit on <i>F</i> <sup>2</sup>	1.078

Crystals included with chloroform were prepared by crystallizing [CuL<sub>2</sub>] (175 mg) from warm chloroform (3.5 g). A 0.4-mm blue oblique block was picked from under the supernatant fluid and frozen quickly to −100 °C to avoid guest escape. Data were collected at −100 °C on a Siemens SMART CCD diffractometer (monochromatic MoK<sub>α</sub> radiation, λ = 0.7107 Å; ω scan mode; 1.6–29° θ-range; −32/32, −32/32, −14/14 *h,k,l*-range). An empirical absorption correction utilized the SADABS routine associated with the Siemens diffractometer.

The structure was solved by direct methods using the SHELX package.<sup>9</sup> Refinement (anisotropic for non-hydrogen atoms) was performed on *F*<sup>2</sup> using all data with positive intensities. Some constraints were applied for the disordered trifluoromethyl group which is rotated about the C(11)–C(12) bond as the group sticks out into the channel (cf. Figures 1 and 11). Host hydrogen atoms were unconstrained, but isotropic thermal factors 1.2 or 1.5 greater than those for adjacent carbon atoms were applied. Guest molecules were given an ideal geometry, whereas thermal parameters were refined anisotropically.

Two symmetrically independent orientations of the guest chloroform were found. Refinement resulted in equal site occupancy factors for both, with a total guest–host ratio of 0.653(6). In the final cycles of refinement, the occupancy for each orientation was fixed to fit a 1/3 guest–host ratio, thus giving a stoichiometry β-[CuL<sub>2</sub>]\*2/3(chloroform). The final *R*-value was 0.034 for 2674 intense data and 263 refined parameters (0.041 for all 3045 data). The only large maximum (0.60 e/Å<sup>3</sup>) remaining in the residual density map was found at the 3̄ site (Wyckoff position *b*).

The structure was analyzed with standard programs.<sup>9,10</sup> Figures were made using the XP<sup>9</sup> and RasMol<sup>11</sup> visualization programs. The channel profiles were outlined using the CLAT program package;<sup>12</sup> the following system of van der Waals radii was applied:<sup>13</sup> C, 1.71; H, 1.16; Cu, 1.40; F, 1.35; O, 1.29 Å.

Salient experimental details and the essential structural parameters are listed in Table 1. Selected geometric parameters for the structure are given in Table 2.

## Results and Discussion

**Sorption Isotherms: General Features.** A number of features become apparent for all isotherms studied, thus disclos-

**TABLE 2: Selected Geometric Parameters for β-[CuL<sub>2</sub>]\*2/3(chloroform)<sup>a</sup>**

bonds	
Cu–O(12)	1.916(1)
Cu–O(14)	1.931(1)
Cu–O(15B)	2.709(1) (intermolecular)
C(11)–F(11)	1.300(2)
C(11)–F(12)	1.294(2)
C(11)–F(13)	1.295(2)
C(11)–C(12)	1.529(3)
C(12)–O(12)	1.267(2)
C(12)–C(13)	1.372(3)
C(13)–C(14)	1.405(3)
C(14)–O(14)	1.256(2)
C(14)–C(15)	1.546(2)
C(15)–O(15)	1.439(2)
C(15)–C(16)	1.506(4)
C(15)–C(17)	1.530(3)
O(15)–C(18)	1.430(3)
all C–Cl	1.707(7)
angles	
O(12)–Cu–O(14)	92.58(5)
O(12)–Cu–O(14A)	87.42(5)
O(12)–Cu–O(15B)	92.92(5)
O(12)A–Cu–O(15B)	87.08(5)
O(14)–Cu–O(15B)	81.92(5)
O(14A)–Cu–O(15B)	98.08(5)
F(11)–C(11)–F(12)	105.9(2)
F(12)–C(11)–F(13)	108.1(2)
F(13)–C(11)–F(11)	105.7(2)
C(12)–C(11)–F(11)	111.2(2)
C(12)–C(11)–F(12)	113.6(2)
C(12)–C(11)–F(13)	118.8(2)
C(11)–C(12)–O(12)	112.2(2)
O(12)–C(12)–C(13)	129.2(2)
C(11)–C(12)–C(13)	118.6(2)
C(12)–O(12)–Cu	123.9(1)
C(12)–C(13)–C(14)	122.1(2)
C(13)–C(14)–O(14)	124.6(2)
O(14)–C(14)–C(15)	116.6(2)
C(13)–C(14)–C(15)	118.7(2)
C(14)–O(14)–Cu	127.2(1)
O(15)–C(15)–C(16)	111.9(2)
O(15)–C(15)–C(17)	104.3(2)
C(16)–C(15)–C(17)	111.0(3)
C(14)–C(15)–O(15)	108.7(2)
C(14)–C(15)–C(16)	110.9(2)
C(14)–C(15)–C(17)	109.8(2)
C(15)–O(15)–C(18)	114.1(2)
all Cl–C–Cl	111.7(6)

<sup>a</sup> Distances, Å; angles, deg; for the numbering scheme see Figure 10. Symmetry transformations: (A) 1–*x*, −*y*, 1–*z*; (B) 4/3–*x*+*y*, 2/3–*x*, −1/3+*z*.

ing important properties that are particular to the host matrix rather than to the guests. The most important conclusion concerns the zeolite-like behavior of the host β-matrix itself as attested by the significant quantities of absorbed guest and the continuity and reversibility of the sorption process. The guest–host ratio of 2/3, a maximum value for this framework, observed for very different systems implies definite stoichiometry; the microstructure of the pores is thus significant, distinctly different from a capillary tube approximation. The similarity of sorption for geometrically analogous molecules (esp. *n*-pentane and diethyl ether) and the dissimilarity observed for chemical analogues (esp. tetrahydrofuran and diethyl ether) underline a physical mode of sorption.

*Continuity* is apparent as sorption starts even at a minimum pressure and continues over the full range of applied guest pressures. This shows that the host material keeps its porosity permanently, even in the absence of included species (at



temperatures below 60 °C). This result is not surprising, as robustness of the empty  $\beta$ -framework was established before by powder X-ray diffraction.<sup>4</sup>

**Reversibility** of sorption is a feature of all the systems studied. Both forward and reverse reactions instantly follow changes in guest pressure. At the same time, completing the processes, especially for sorption, in some cases requires hours. The most probable explanation concerns guest size. For example, the rate of desorption drops dramatically on going from methylene chloride through chloroform to carbon tetrachloride. Figure 1 confirms the relation between this observation and the capability of a guest to move along the channel. Such "braking kinetics" might also have thermodynamic origins, as guest–guest interactions result in a decrease in isosteric heat of sorption with the filling of available cavity space.<sup>8</sup>

The *quantity of absorbed guest* is significant; for most systems studied up to 2/3 mol of guest/mol of host are included. This implies a stoichiometric filling of both sorption sites. In mass percent, the maximum quantities of absorbed guest were as follows: methylene chloride, 11.7; chloroform, 17.5; carbon tetrachloride, 20.6; *n*-pentane, 6.9; acetone, 8.4; tetrahydrofuran, 9.9; diethyl ether, 7.2.

**Isotherm shape.** All isotherms were type I in Brunauer's classification.<sup>14</sup> This type is characteristic of solids containing micropores.<sup>15</sup> Enhanced sorption in micropores causes a sharp rise of the isotherm on passing to a plateau corresponding to saturation values. Characteristically, these values depend only weakly on temperature. The absence of inflection points in the early parts of the isotherms is consistent with the low flexibility of the  $\beta$ -[CuL<sub>2</sub>];<sup>4</sup> very likely all pore space is permanently available and the sorption does not generate additional sorption sites, a phenomenon characteristic of some highly flexible host matrices.<sup>1,16</sup>

The isotherms studied reveal a *physical mode of sorption*; they are well-described by a Langmuir equation written as

$$x = x_{\max} \frac{KP_{\text{guest}}}{1 + KP_{\text{guest}}}$$

where  $x$  is an equilibrium (absorbed guest)–(host sorbent) mole ratio at a guest pressure  $P_{\text{guest}}$ ,  $x_{\max}$  is the maximum value of  $x$ , and  $K$  is a sorption constant. Figure 3 illustrates the linear dependence  $P_{\text{guest}}/x = (1/x_{\max}K) + (P_{\text{guest}}/x_{\max})$  as a function  $P_{\text{guest}}/x(P_{\text{guest}})$

Derived from this,  $x_{\max} = 0.676(5)$  and  $K = 0.12(1)$  (mmHg)<sup>−1</sup>. Assuming that each methylene chloride molecule occupies an area  $\sigma = 45 \text{ \AA}^2 = 45 \times 10^{20} \text{ m}^2$  on a surface, the specific surface area<sup>15</sup> would be

$$\frac{x_{\max} N_A}{M} \sigma = 377 \text{ m}^2/\text{g}$$

( $N_A = 6.023 \times 10^{23}$  molecules/mol is the Avogadro constant,  $M = 485.9 \text{ g/mol}$  is the molar mass of [CuL<sub>2</sub>] host).  $\beta$ -[CuL<sub>2</sub>] therefore is equivalent to an adsorbent with surface area of 377 m<sup>2</sup>/g with respect to methylene chloride.

**Sorption Isotherms: Specifics.** For methylene chloride, chloroform, and carbon tetrachloride (Figures 2, 4, and 5), the isotherms below 60 °C rise quickly, approaching guest–host mole ratio values of ca. 2/3 even at a guest pressure of 10–20 mmHg. The chloroform isotherm is significantly sharper than that for methylene chloride. This is consistent both with the lower volatility of chloroform and its better complementarity to the channel dimensions (see Figure 1).

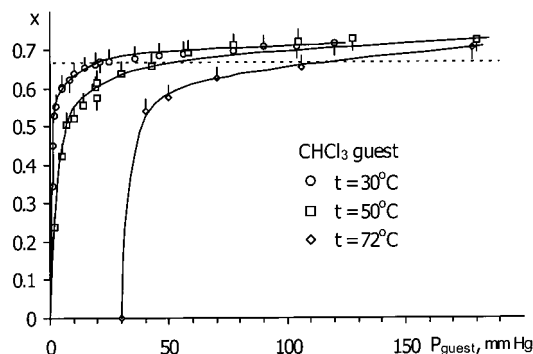


**Figure 4.** Sorption isotherms for chloroform in  $\beta$ -[CuL<sub>2</sub>] over a range of temperatures. The point ( $P = 30$ ;  $x = 0$ ) for the 72 °C isotherm is consistent with a collapse of the host porous  $\beta$ -matrix to the dense  $\alpha$ -form (see text).

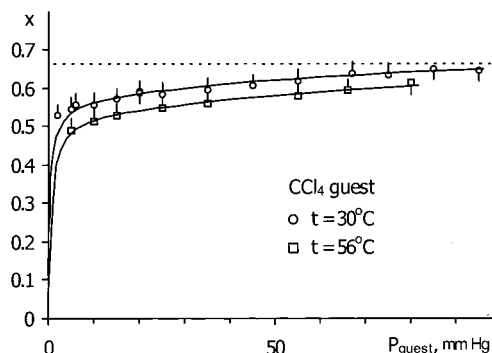


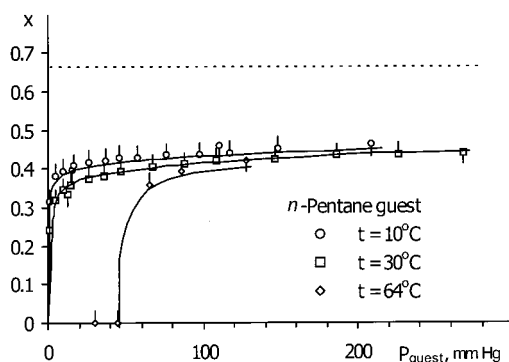
**Figure 5.** Sorption isotherms for carbon tetrachloride in  $\beta$ -[CuL<sub>2</sub>] at 30 and 56 °C.

For chloroform, the isotherm at 72 °C turns down sharply to  $x \sim 0$  near a guest pressure of 30 mmHg. This suggested a complete loss of microporosity under the conditions applied, and we suggest that the  $\beta$ -matrix collapses into the dense,  $\alpha$ -polymorph of the complex. To confirm this, a sample of the chloroform  $\beta$ -inclusion was placed in an air-free cell at 72 °C under a methylene chloride pressure of ca. 30 mmHg. During the second hour of exposure, the pressure increased with auto-acceleration to a value of ca. 140 mmHg; after pumping down to 30 mmHg again and holding this pressure for the next hour, the recovered sample indeed was found to be pure  $\alpha$ -form. This experiment defines the range of conditions over which the  $\beta$ -matrix may be used. The results on collapse of empty  $\beta$ -matrix are described in the next part.

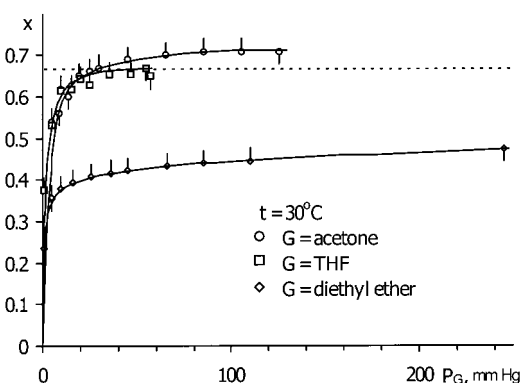
The *n*-pentane isotherms at 10 and 30 °C rise very sharply to  $x \sim 0.44$ , the value that corresponds well to that from isopiestic measurements<sup>5</sup> and indicates that guest sorption is essentially nonstoichiometric. The most probable model here has a dense filling of the channel with guest species, as found before for the inclusion with *n*-hexane.<sup>5</sup> The isotherm at 64 °C drops down at ca. 45 mmHg, indicating collapse to the nonporous  $\alpha$ -form as noted above for chloroform.

Figure 7 summarizes data on the sorption of oxygen-containing species. Acetone and tetrahydrofuran are absorbed to stoichiometric values (some systematic excess for acetone is likely to be due to surface adsorption), whereas diethyl ether behaves like *n*-pentane. Thus, within the range of guests studied, the geometric factor turns out to be more decisive than polarity or chemical analogy.

**Conversion and Energy Relations between  $\alpha$ - and  $\beta$ -Polymorphs.** The  $\alpha$ -form is the stable polymorph of the [CuL<sub>2</sub>] complex and thus it cannot transform directly to the metastable



**Figure 6.** Sorption isotherms for *n*-pentane in  $\beta$ -[CuL<sub>2</sub>] over a range of temperatures. The points at  $x = 0$  on the 64 °C isotherm are consistent with a collapse of the  $\beta$ -matrix (cf. Figure 4).



**Figure 7.** Sorption isotherms (30 °C) for acetone, tetrahydrofuran, and diethyl ether in  $\beta$ -[CuL<sub>2</sub>].

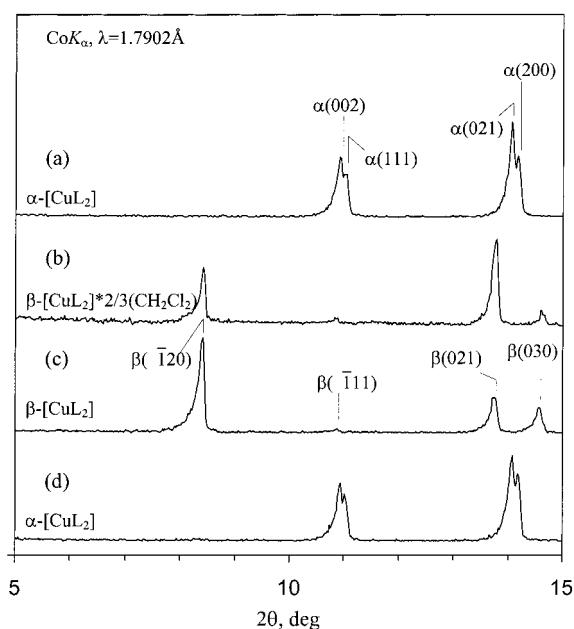


**Figure 8.** Selected powder diffractograms: (a) [CuL<sub>2</sub>] complex after sublimation, pure  $\alpha$ -form; (b) the same sample exposed to methylene chloride vapor (ca. 300 mmHg, 5 h); an increase in mass and the reflections shown indicate the formation of the  $\beta$ -inclusion,  $\beta$ -[CuL<sub>2</sub>]\*2/3(CH<sub>2</sub>Cl<sub>2</sub>); (c) sample from trace b after evacuation (12 h, down to  $10^{-5}$  mmHg); the diffractogram shows preservation of the  $\beta$ -matrix after guest removal (with a guest residue of less than 0.1 mass.%); (d) sample from trace c after heating for 20 min at 70 °C shows complete collapse to  $\alpha$ -form.

$\beta$ -form. The transformation is possible through formation of an inclusion compound with a suitable templating guest that stabilizes the  $\beta$ -matrix sufficiently. Removing the template

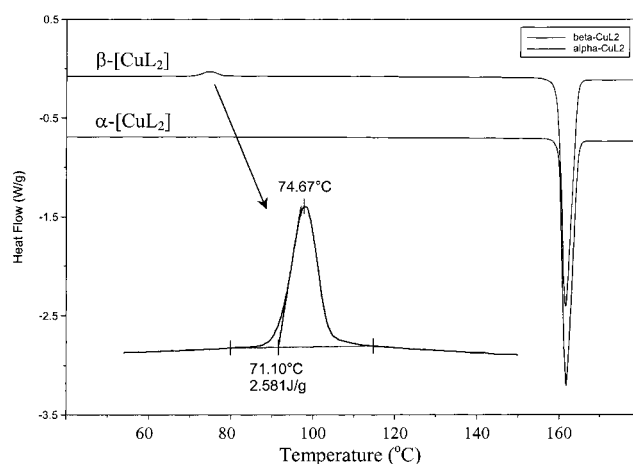


**Figure 9.** Differential scanning calorimetry curves for the two polymorphs of [CuL<sub>2</sub>]. The exotherm corresponding to the  $\beta \rightarrow \alpha$  collapse also is shown separately on an enlarged scale.

**TABLE 3: Phase Transitions for  $\alpha$ - and  $\beta$ -polymorphs of [CuL<sub>2</sub>] Complex from DSC**

initial sample	no. of exp	$t$ , °C	heat effect, kJ/mol	assigned process
$\beta$ -[CuL <sub>2</sub> ]	6	70.0(8)	1.31(5) <sup>a</sup> , exo	$\beta \rightarrow \alpha$
		160.1(2)	40.5(2), endo	$\alpha = \text{liquor}$
$\alpha$ -[CuL <sub>2</sub> ]	5	160.1(3) <sup>b</sup>	40.8(3), endo	$\alpha = \text{liquor}$

<sup>a</sup> Assuming the process occurs completely in 20° range (cf. Figure 9). <sup>b</sup> Visually observed melting point of 157–158 °C was reported.<sup>4</sup>

results in the empty  $\beta$ -form. At the same time, the  $\beta$ -to- $\alpha$  collapse is energetically favorable and may occur spontaneously as soon as the kinetic barrier is overcome. Figure 8 illustrates the above interconversions. The  $\alpha$ -form (a) produces the  $\beta$ -inclusion when exposed to a methylene chloride atmosphere (b). The guest template is then removed to give the empty microporous  $\beta$ -matrix (c). Short-term heating induces its collapse to the original  $\alpha$ -form (d).

The comparison of DSC-curves for  $\alpha$ - and  $\beta$ -polymorphs (Figure 9) reveals the following important features. In the temperature range studied, the  $\alpha$ -form shows only an endotherm of 40.8(3) kJ/mol at 160 °C corresponding to congruent melting. The DSC-curve of the  $\beta$ -form sample shows two effects, one being identical to the  $\alpha$ -form melting transition (Table 3, Figure 9). Another thermal effect at 70 °C is exothermic and suggests the presence of a nonequilibrium phase transition, that is, the collapse, of the  $\beta$ -phase to the stable  $\alpha$ -modification. Surprisingly, the process occurs over a narrow range, the effect being very pronounced and symmetrical in shape. This may imply a chain mechanism for the  $\beta$ -to- $\alpha$  phase restructuring. According to our previous study,<sup>4</sup> this process should occur in at least two steps: the first proceeds on a molecular level and is the trans-cis isomerization of the [CuL<sub>2</sub>] unit. The second step, which occurs on a supramolecular level, involves the reassembly of [CuL<sub>2</sub>] units into a new coordination polymer framework. The isomerization process behaves as a switch enabling supramolecular reassembly, while the latter may provide feedback that accelerates the isomerization and thereby the whole process.

Integration of the  $\beta$ -to- $\alpha$  exotherm (Table 3) directly gives an energy difference of 1.31(5) kJ/mol for the polymorphs:

$$\beta\text{-[CuL}_2\text{]} = \alpha\text{-[CuL}_2\text{]} + 1.31(5) \text{ kJ/mol (at 70 °C)} \quad (3)$$

The effect is small, thus explaining the high affinity of the complex for the open form. This value may be compared with that for the [Ni(4-MePy)<sub>4</sub>(NCS)<sub>2</sub>] host, though both microporous

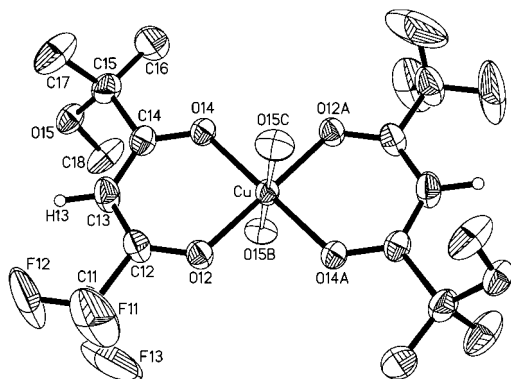


**Figure 10.** Host molecule coordinated by oxygen atoms of neighboring hosts in  $\beta$ -[CuL<sub>2</sub>]\*2/3(chloroform). A-labeled atoms are generated through centrosymmetry, O(15B) and O(15C) with  $(4/3-x+y, 2/3-x, -1/3+z)$  and  $(-1/3+x-y, -2/3+x, 4/3-z)$  operators, respectively. Methyl hydrogen atoms are omitted.

( $\beta$ )<sup>17</sup> and dense ( $\alpha$ )<sup>18</sup> polymorphs of the complex are based only on van der Waals interactions, the  $\alpha$ -to- $\beta$  conversion requires 3.5(1) kJ/mol,<sup>19</sup> and this value should be doubled to dilate the flexible  $\beta$ -framework to include molecules such as benzene.<sup>20</sup> The enthalpy for the  $\alpha$ -to- $\beta$  transformation of 0.5(1) kJ/mol for hydroquinone<sup>21</sup> is in fact more significant in terms of energy per mass unit, as the molar mass of hydroquinone (110.1) is a factor of 4 less than that of [CuL<sub>2</sub>] (485.9).

**Crystal Structure of the Chloroform Inclusion.** The single-crystal X-ray diffraction study confirms the inclusion character and accounts for the ideal stoichiometry of the compound with chloroform, formulated as  $\beta$ -[CuL<sub>2</sub>]\*2/3(chloroform). Like other  $\beta$ -inclusions of the title host, the structure consists of 3D assembled, electrically neutral [CuL<sub>2</sub>] units and guest species included in 1D channel.

An ORTEP drawing of the host unit is shown in Figure 10. It is centrosymmetric and thus is trans-configured. The copper(II) center is in the square-planar environment of four oxygen donors from two deprotonated acetylacetone units acting as bidentate ligands with Cu–O distances of 1.92–1.93 Å.

The copper coordination becomes complete because of the apical methoxy oxygens donated by neighboring molecules at a distance of 2.709(1) Å. The same value was found previously for inclusion with *n*-hexane,<sup>5</sup> whereas for three other inclusions this bond was longer: 2.800(2) Å with benzene,<sup>4</sup> 2.738(2) Å with *tert*-butyl alcohol,<sup>5</sup> and 2.786(2) Å with *tert*-butylbenzene.<sup>6</sup> This is because the peripheral methoxy oxygen may also participate in intramolecular hydrogen bonding to the C–H group of the chelate ring. This bimodal connectivity seems to be responsible for the slight flexibility of the  $\beta$ -matrix and thus for the geometry of the channel. In the chloroform inclusion, the C(13)–O(15) distance of 2.900(2) Å is comparable to that in the *n*-hexane inclusion but longer than in the other three. Inclusions with chloroform and *n*-hexane thus maintain a

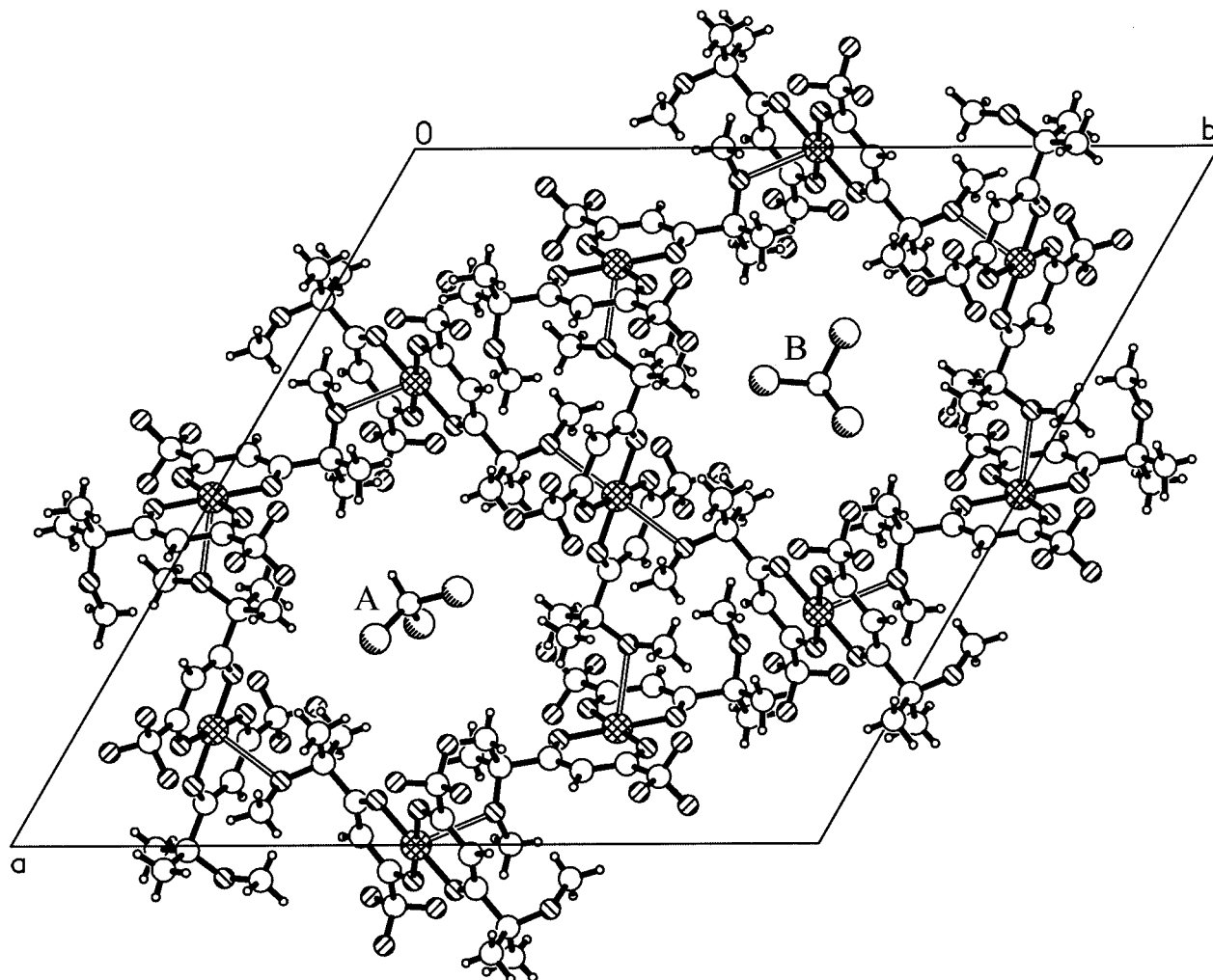


**Figure 11.** Molecular assembly and packing in  $\beta$ -[CuL<sub>2</sub>]\*2/3(chloroform). Projection of the host framework is shown along the channel direction along with the included guest species. For clarity, two independent orientations of the guest molecules are shown in different channels and all symmetrical equivalents are suppressed.



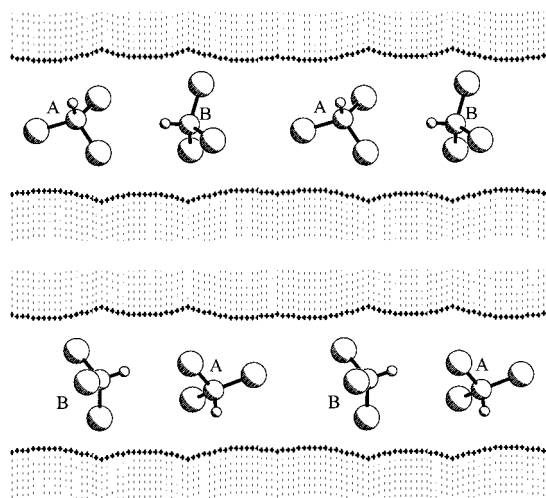


**Figure 12.** Possible variants of guest chloroform ordering in the 1D channel of the host matrix. Channel segments of two periods each are shown.

situation of stronger coordinative assembly to the detriment of weaker intramolecular bonding. This results in a smoother channel, with a minimal change in the channel diameter of 5.14–5.98 Å (cf. 4.85–6.36 Å for inclusion with *tert*-butylbenzene<sup>6</sup>).

Figure 11 shows the 3D host assembly with the channels lying along the *c* crystallographic axis. The inner surface of the channel is composed of methyl and trifluoromethyl host moieties. Guest chloroform species in two unequivalent orientations are shown in two different channels for clarity. For the A-oriented guest the C–H bond is almost perpendicular to the channel axis, whereas for the B-oriented guest it is nearly parallel.

The A-oriented guest cannot fill the channel stoichiometrically, as this would result in overlapping chlorine atoms. At the same time, alternation of A- and B-oriented molecules along the channel axis allows stoichiometric filling, fully consistent with the 1:1 ratio found experimentally. The profile of the channel and the suggested mode of alternating guest orientations is shown in Figure 12. The A-guest fills the small cavity, whereas the B-guest sits mainly in the large cavity. An analogous situation, with two guest orientations in a 1:1 ratio and an overall 2/3 guest–host stoichiometry also was observed for the benzene inclusion.<sup>4</sup>

The structure studied may well illustrate the stoichiometric mode of filling for the compact molecules studied in this work in general. The nature of the compound with tetrahydrofuran may well be like that with benzene. Inclusions with *n*-pentane and diethyl ether are essentially nonstoichiometric and are unlikely to exhibit long-range order of the guests. At low temperatures, they may well show dense guest packing with a long periodicity or show the incommensurate character characteristic of tubulates formed by urea.<sup>22</sup> Another option is the preferred filling of large cavities, with partial filling of small cavities, characteristic of clathrate hydrates<sup>23</sup> and trigonal Werner hosts.<sup>24,25</sup>

**Acknowledgment.** Part of this work was carried out within the scope of a collaborative project between the Institute of Inorganic Chemistry, Siberian Branch of the Russian Academy of Sciences and the Institute of Physical Chemistry, Polish Academy of Sciences. D.V.S. is grateful for a Visiting Fellowship at the Steacie Institute for Molecular Sciences, National Research Council Canada. We thank Prof. Yu. A. Dyadin for

his support and interest in this work and Dr. V. V. Tersikh for alerting us to some relevant literature.

**Supporting Information Available:** Final fractional atomic coordinates and other structural data for  $\beta$ -[CuL<sub>2</sub>] $\cdot$ 2/3(chloroform). This material is available free of charge via the Internet at <http://pubs.acs.org>.

## References and Notes

- (1) Allison, S. A.; Barrer, R. M. *J. Chem. Soc. A* **1969**, 1717–1723.
- (2) (a) Lipkowski, J. In *Inclusion Compounds*, Atwood, J. L., Davies, J. E. D., MacNicol, D. D., Eds.; Academic: London, 1984; Vol. 1, pp 59–103. (b) Ung, A. T.; Gizachew, D.; Bishop, R.; Scudder, M. L.; Dance, I. G.; Craig, D. C. *J. Am. Chem. Soc.* **1995**, *117*, 8745–8756. (c) Venkataraman, D.; Gardner, G. B.; Lee, S.; Moore, J. S. *J. Am. Chem. Soc.* **1995**, *117*, 11600–11601. (d) In *Comprehensive Supramolecular Chemistry*; MacNicol, D. D., Toda, F., Bishop, R., Eds.; Pergamon: Oxford, 1996; Vol. 6 (see Mak, T. S. W., Bracke, B. R. F., p 39; Gdanec, M., Ibragimov, B. T., Talipov, S. A., pp 139–140; Lipkowski, J., pp 697–698). (e) Yaghi, O. M.; Li, G.; Li, H. *Nature* **1995**, *378*, 703–706. (f) Kondo, M.; Yoshitomi, T.; Seki, K.; Matsuzaka, H.; Kitagawa, S. *Angew. Chem., Int. Ed. Engl.* **1997**, *36*, 1725–1727. (g) Brunet, P.; Simard, M.; Wuest, J. D. *J. Am. Chem. Soc.* **1997**, *119*, 2737–2738. (h) Russel, V. A.; Evans, C. C.; Li, W.; Ward, M. D. *Science* **1997**, *276*, 575–579. (i) Kepert, C. J.; Rosseinsky, M. J. *Chem. Commun.* **1999**, 375–376. (j) Li, H.; Eddaoudi, M.; O’Keeffe, M.; Yaghi, O. M. *Nature* **1999**, *402*, 276–279.
- (3) Partially crystalline and glassy organic polymers are another class of microporous solids revealing zeolite-like properties: (a) Ichiraku, Y.; Stern, S. A.; Nakagawa, T. *J. Membr. Sci.* **1987**, *34*, 5–18. (b) Witchey-Lakshmanan, L. C.; Hopfenberg, H. B.; Chern, R. T. *J. Membr. Sci.* **1990**, *48*, 321–331. (c) Volkov, V. V. *Polim. J.* **1991**, *23*, 457–466. (d) Srinivasan, R.; Auvil, S. R.; Burban, P. M. *J. Membr. Sci.* **1994**, *86*, 67–86. (e) Ilinitich, O. M.; Fenelonov, V. B.; Lapkin, A. A.; Okkel, L. G.; Tersikh, V. V.; Zamaraev, K. I. *Microp. Mesop. Mater.* **1999**, *31*, 97–110.
- (4) Soldatov, D. V.; Ripmeester, J. A.; Shergina, S. I.; Sokolov, I. E.; Zanina, A. S.; Gromilov, S. A.; Dyadin, Yu. A. *J. Am. Chem. Soc.* **1999**, *121*, 4179–4188.
- (5) Soldatov, D. V.; Ripmeester, J. A. *Chem. Mater.* **2000**, *12*, 1827–1839.
- (6) Soldatov, D. V.; Ripmeester, J. A. *J. Incl. Phenom.* in press.
- (7) Barbour, L. J.; Achleitner, K.; Greene, J. R. *Thermochim. Acta* **1992**, *205*, 171–177.
- (8) Manakov, A. Yu.; Lipkowski, J. *J. Incl. Phenom.* **1997**, *29*, 41–55.
- (9) Sheldrick, G. M. *SHELXTL PC, Ver. 4.1. An Integrated System for Solving, Refining and Displaying Crystal Structure from Diffraction Data*; Siemens Analytical X-ray Instruments, Inc.: Madison, WI, 1990.
- (10) Barbour, L. J.; Atwood, J. L. *J. Appl. Crystallogr.* **1998**, *31*, 963–964.
- (11) Sayle, R.; Milner-White, E. J. *RasMol: Biomolecular Graphics for All, Trends in Biochemical Sciences (TIBS)*, September, 1995; Vol. 20, No. 9, p 374.
- (12) Grachev, E. V.; Dyadin, Yu. A.; Lipkowski, J. *J. Struct. Chem.* **1995**, *36*, 876–879.
- (13) Zefirov, Yu. V.; Zorkii, P. M. *Russ. Chem. Rev.* **1995**, *64*, 415–428.
- (14) Brunauer, S. *The Adsorption of Gases and Vapors*, Princeton University Press: Princeton, N.J., 1943; Vol. I.
- (15) Webb, P. A.; Orr, C. *Analytical Methods in Fine Particle Technology*, Micromeritics Instrument Corporation, Norcross, GA, 1997; Chapter 3.
- (16) Lipkowski, J.; Majchrzak, S. *Rocz. Chem.* **1977**, *49*, 1655–1660.
- (17) Kerr, I. S.; Williams, D. J. *Acta Crystallogr.* **1977**, *B33*, 3589–3592.
- (18) Andreotti, G. D.; Bocelli, G.; Sgarabotto, P. *Cryst. Struct. Commun.* **1972**, *1*, 51–54.
- (19) Lipkowski, J.; Chajn, J. *Rocz. Chem.* **1977**, *51*, 1443–1448.
- (20) Lipkowski, J.; Starzewski, P.; Zelenkiewicz, W. *Thermochim. Acta* **1977**, *49*, 269–279.
- (21) Evans, D. F.; Richards, R. E. *J. Chem. Soc.* **1952**, 3932–3936.
- (22) (a) Hollingsworth, M. D.; Harris, K. D. M. In *Comprehensive Supramolecular Chemistry*; MacNicol, D. D., Toda, F., Bishop, R., Eds.; Pergamon: Oxford, 1996; Vol. 6, pp 177–237. (b) Brown, M. E.; Chaney, J. D.; Santarsiero, B. D.; Hollingsworth, M. D. *Chem. Mater.* **1996**, *8*, 1588–1591.
- (23) (a) McMullan, R. K.; Jeffrey, G. A. *J. Chem. Phys.* **1965**, *42*, 2725–2732. (b) Glew, D. N.; Rath, N. S. *J. Chem. Phys.* **1966**, *44*, 1710–1711. (c) Ripmeester, J. A.; Davidson, D. W. *J. Mol. Struct.* **1981**, *75*, 67–72. (d) Jeffrey, G. A. In *Inclusion Compounds*, Atwood, J. L., Davies, J. E. D., MacNicol, D. D., Eds.; Academic: London, 1984; Vol. 1, pp 135–190.



(e) Dyadin, Yu. A.; Bondaryuk, I. V.; Aladko, L. S. *J. Struct. Chem.* **1995**, *36*, 995–1045.

(24) (a) Soldatov, D. V.; Trushin, P. A.; Logvinenko, V. A.; Grachev, E. V. *J. Struct. Chem.* **1993**, *34*, 232–238. (b) Lipkowski, J.; Soldatov, D. V. *J. Incl. Phenom.* **1994**, *18*, 317–329.

(25) For recent examples on guest distribution over different sorption sites in channels of a Werner complex  $\beta$ -phase, see also (a) Lavelle, L.; Nassimbeni, L. R. *J. Incl. Phenom.* **1993**, *16*, 25–54. (b) Manakov, A. Yu.; Lipkowski, J.; Suwinska, K.; Kitamura, M. *J. Incl. Phenom.* **1996**, *26*, 1–20.